J Comp Physiol A (1990) 166:489–499

Journal of Comparative Physiology A Sensory, Neural, and Behavioral Physiology

Encoding of a spectrally-complex communication sound in the bullfrog's auditory nerve

Joshua J. Schwartz and Andrea Megela Simmons

Department of Psychology, Brown University, Providence, Rhode Island 02912, USA

Accepted October 14, 1989

Summary. 1. A population study of eighth nerve responses in the bullfrog, *Rana catesbeiana*, was undertaken to analyze how the eighth nerve codes the complex spectral and temporal structure of the species-specific advertisement call over a biologically-realistic range of intensities. Synthetic advertisement calls were generated by Fourier synthesis and presented to individual eighth nerve fibers of anesthetized bullfrogs. Fiber responses were analyzed by calculating rate responses based on post-stimulus-time (PST) histograms and temporal responses based on Fourier transforms of period histograms.

2. At stimulus intensities of 70 and 80 dB SPL, normalized rate responses provide a fairly good representation of the complex spectral structure of the stimulus, particularly in the low- and mid-frequency range. At higher intensities, rate responses saturate, and very little of the spectral structure of the complex stimulus can be seen in the profile of rate responses of the population.

3. Both AP and BP fibers phase-lock strongly to the fundamental (100 Hz) of the complex stimulus. These effects are relatively resistant to changes in stimulus intensity. Only a small number of fibers synchronize to the low-frequency spectral energy in the stimulus. The underlying spectral complexity of the stimulus is not accurately reflected in the timing of fiber firing, presumably because firing is 'captured' by the fundamental frequency.

4. Plots of average localized synchronized rate (ALSR), which combine both spectral and temporal information, show a similar, low-pass shape at all stimulus intensities. ALSR plots do not generally provide an accurate representation of the structure of the advertisement call.

5. The data suggest that anuran peripheral auditory fibers may be particularly sensitive to the amplitude envelope of sounds.

Key words: Frog – Periodicity – Communication – Neuroethology – Auditory nerve

Introduction

The male bullfrog, *Rana catesbeiana*, employs several functionally-distinct vocalizations for communication with conspecifics (Capranica 1968; Wiewandt 1969). These vocalizations, which include advertisement, territorial, warning, and release calls, consist of multiple harmonically-related frequencies with waveform periodicities ranging from 30 Hz to 100 Hz. Variations in both the spectral and the temporal structure of these conspecific signals may be used by the bullfrog to distinguish among the different calls in its repertoire (Capranica 1968). Moreover, male bullfrogs are able to distinguish between the advertisement calls of neighbors and strangers on the basis of acoustic characteristics (Davis 1987).

The peripheral auditory system of the bullfrog, as well as other anurans, is specialized to detect species-specific communication sounds. The inner ear of these animals contains two organs specialized for reception of sounds. Neither of these organs contains a basilar membrane. One organ, the amphibian papilla (AP), is tonotopically organized and tuned to low frequencies in the range of 100–1000 Hz (Lewis et al. 1982). The tuning of the bullfrog's AP overlaps the low-frequency spectral energy present in its communication sounds (peaks at 200–300 Hz in the advertisement call and peaks at 500–800 Hz in the territorial call; Capranica 1968). The other organ, the basilar papilla (BP), operates as a resonant organ tuned to a higher range of frequencies, from about 1000–2000 Hz in the bullfrog (Feng et al. 1975; Freedman et al. 1988). This high frequency range encompasses the high-frequency spectral energy present in the advertisement call. The tuning of the BP is species-specific; BP fibers in anurans with higher frequency

Abbreviations: *ALSR* average localized synchronized rate; *AP* amphibian papilla; *BP* basilar papilla; *CF* characteristic frequency

components in their vocalizations generally are tuned to these higher frequencies. This overlap between the frequency composition of biologically-relevant vocal signals and the tuning of the two papillae has led to the hypothesis that the anuran's peripheral auditory system acts as a sort of 'matched filter' for processing of spectral features in species-specific vocalizations (Capranica and Moffat 1983).

The 'matched filter' hypothesis has generated a good deal of research analyzing both frequency and temporal coding of sounds in the anuran's eighth nerve. Much of this research has focused on responses to relatively simple stimuli such as tone bursts, two-tone complexes, or amplitude modulated tones and noise (see Zakon and Wilczynski 1988, for a recent review). It is difficult to extrapolate, however, from fiber responses to these relatively simple stimuli to the types of spectrally- and temporally-complex stimuli an animal must perceive in its natural environment. The issue of how the anuran auditory periphery codes complex signals that vary both spectrally and temporally, as natural vocalizations do, has not been adequately approached. Moreover, anurans typically communicate at high intensity levels (80–90 dB SPL at distances of 1 m for the bullfrog; Megela-Simmons 1984). These levels exceed the linear dynamic range of many individual eighth nerve fibers (Capranica and Moffat 1983; Feng 1982; Narins 1987). Although a process of range fractionation (Feng 1982; Narins 1987) may operate for coding of different intensities of pure tones, it has not been established how the eighth nerve responds to complex vocal signals at biologically-realistic intensities.

An area of active research in mammalian auditory neurophysiology concerns how spectral, temporal, and intensity information in a complex stimulus (such as synthetic speech sounds) are encoded over a wide dynamic range (Delgutte and Kiang 1984a, b; Miller and Sachs 1983; Sinex and Geisler 1983; Young and Sachs 1979). Two general schemes are available for processing the structure of harmonically-complex signals. One is by a rate-place code (average rate across best frequency), in which fibers fire at rates which increase with increases in energy in their tuning curves (Sachs and Young 1979). The other is by a temporal-place code (phase-locking across best frequency), in which fibers fire at particular points in the cycles of components of the complex stimulus and so preserve the period of these components (Young and Sachs 1979). The mammalian eighth nerve utilizes both schemes. A temporal-place representation can encode features of synthetic speech sounds at both stimulus and background noise intensities that produce saturation in rate responses (Delgutte and Kiang 1984a; Miller and Sachs 1983, 1984; Sachs et al. 1983; Sinex and Geisler 1983; Young and Sachs 1979). A rate-place code is important for coding features of consonant-vowel syllables and of vowel sounds at low stimulus intensities (Delgutte and Kiang 1984b; Geisler and Gamble 1989; Miller and Sachs 1983; Sinex and Geisler 1983).

We set out to investigate how the bullfrog's auditory nerve encodes the acoustic features and complex structure in the advertisement call over a biologically-meaningful range of intensities. Our strategy was to record responses from a population of fibers to a single, stereotyped stimulus over a wide range of intensities. We were particularly interested in comparing the operation of spectral and temporal coding schemes for representing complex spectral structure in a robust way. Moreover, we wished to determine whether the peculiar anatomical division of the anuran inner ear into two discrete organs would manifest itself in response properties and coding strategies different from those observed in higher vertebrates.

Materials and methods

Adult bullfrogs (200–400 g), obtained from a commercial supplier, were anesthetized by intramuscular injections of sodium pentobarbitol (Nembutal; 100 mg/kg) for both surgery and recording. The animals were kept moist with wet gauze throughout the experiment to aid cutaneous respiration. The eighth nerve was exposed via a ventral approach through the roof of the mouth. The animal was positioned on a vibration isolation table (Newport Research Corp.) in a sound attenuating chamber (Industrial Acoustics). Stimulus generation and recording equipment were located outside the chamber. Experiments were conducted at room temperature (approximately 20° C).

Acoustic stimuli were presented ipsilateral to the exposed nerve with a calibrated closed field acoustic stimulation system. This system consisted of a Beyer DT48 earphone enclosed in a custom-built brass housing with a symmetrical T-shaped coupler (50 mm length, 13 mm diameter) attached to its face. One end of the coupler contained a Brüel and Kjaer 4134 1/2″ condenser microphone for monitoring the sound pressure level (dB SPL re: 20 μPa) of the stimulus. The other end of the T was fit with a tapered rubber tube which was placed close to, but not touching, the animal's tympanum. The rubber tube was sealed around the edges of the tympanum with silicone grease to form a closed system. The frequency response of the coupling system was calibrated using the 1/2″ microphone and a Brüel and Kjaer 2209 sound level meter, and adjusted with a Rane stereo equalizer to be flat (±4 dB) over the range of 100–5000 Hz. For analysis, sounds were digitized with an R/C Electronics isc-16 interface board and spectra were computed with an IBM PC/XT computer using ILS programs from Signal Technology, Inc.

Synthetic advertisement calls with 21 components, derived from waveforms and sonagrams presented by Capranica (1965), were digitally constructed on an IBM PC/XT computer using Fourier synthesis. The frequency components in the synthetic call were all in sine phase. Digital-to-analog conversion was accomplished with a Data Translation 2801A board at a sampling rate of 10 kHz. The signal had a bimodal spectrum, with a low-frequency peak around 200–300 Hz, a dip in the frequency region around 500 Hz, a broad high-frequency peak around 1400–1500 Hz, and a periodicity of 100 Hz (Fig. 1). Distortion products in the stimulus were at least 72 dB down at the frog's ear. Stimulus duration was 800 ms and rise/fall time was 10 ms. The stimuli were low-pass filtered (Krohn-Hite model 3550) at 5 kHz, attenuated (Coulbourn S85-08 electronic attenuator), amplified (Harmon/Karden PM 645 stereo amplifier) and presented to the animal as described above.

Activity of single eighth nerve fibers was recorded with 3 *M* KCL-filled glass micropipettes of 30–60 MΩ impedance. The micropipettes were advanced into the nerve by a remotely-controlled hydraulic microdrive (Kopf model 607). Neuronal responses were first amplified by a WPI DAM 80 AC differential amplifier (gain of 1000, band-pass filtered at 10 Hz-3 kHz), and then amplified and filtered by a Rockland 442 filter (gain of 20 dB, filtered at

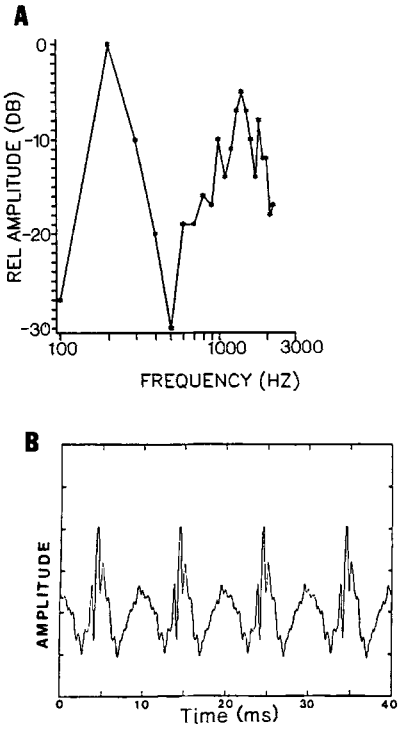

Fig. 1. **A** Amplitude-frequency display of the 21 component synthetic advertisement call. Each point represents one of the 21 harmonic components. Note the relatively small amount of energy at 100 Hz, the fundamental frequency. **B** Amplitude-time display of the stimulus near the frog's tympanum, to illustrate the periodicity

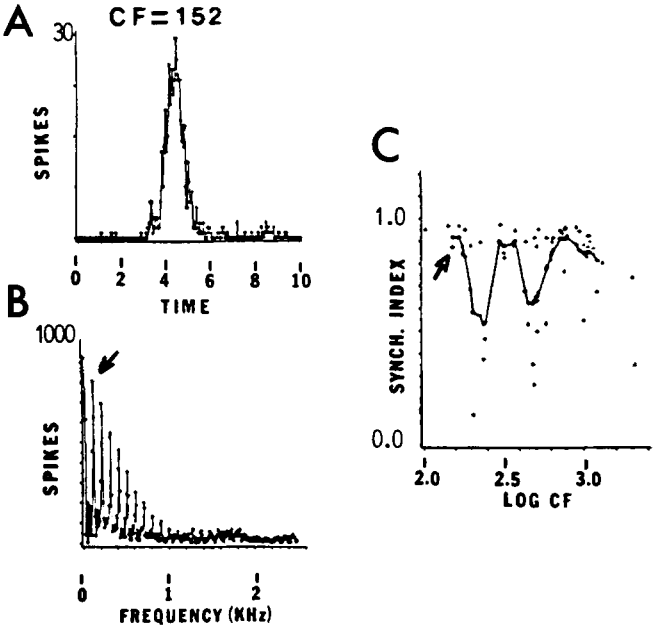

Fig. 2. Example of the steps used to calculate the synchronization index. **A** Period histogram, compiled over a 10 ms period, of a fiber's (CF = 152 Hz) responses to presentations of the synthetic advertisement call at 80 dB. **B** Fourier transform of 5 cycles of this period histogram; arrow indicates the 100 Hz peak. **C** Plot of the synchronization index to 100 Hz of all fibers recorded at 80 dB SPL against CF; arrow indicates the position of the data point for the 152 Hz fiber. The solid line through the data points represents a moving average computed with a triangular weighting function with a 0.5 octave base

0.3–3 kHz). They were displayed on an oscilloscope (Tektronix 922R), monitored over a loudspeaker, and recorded on one channel of a TEAC quadrophonic tape recorder for subsequent analysis. The complex stimulus and a computer-generated pulse coincident with stimulus onsets were simultaneously recorded on two other channels of the tape recorder.

The search stimulus was a frequency-modulated sweep (50 Hz–3 kHz, sweep rate 1/s, presented at a level of 80 dB SPL) generated by one Wavetek model 182 function generator sweeping another. Once an auditory fiber was encountered, its spontaneous activity, characteristic frequency to pure tones (CF), and threshold at both CF and to the synthetic call were measured. Threshold was estimated as the elevation in spike rate above spontaneous activity which was just audible (audio monitor) and visible (oscilloscope). Anuran eighth nerve fibers exhibit little or no spontaneous activity (0–30 spikes/s, with the majority of fibers having rates of 0–5 spikes/s; Megela and Capranica 1981; Zelick and Narins 1985), making estimates of increases above spontaneous rate fairly straightforward. Synthetic calls were then presented at a series of increasing intensities (generally, over the range of 70–100 dB SPL or until the fiber reached rate saturation) at a repetition rate of 1/2 s, for at least 30 repetitions.

Spike counts, peri-stimulus-time (PST) histograms and period histograms were calculated with an IBM PC/AT computer and R/C Electronics data acquisition board and accompanying software. Data were sampled at a rate of 20 kHz (50 μs bin width). As a measure of rate (spectral) responses of the fibers, plots of spike discharge rate over fiber CF in response to the complex stimulus were compiled, separately for each intensity level. Discharge rate was normalized by subtracting spontaneous rate and then dividing by (saturation rate − spontaneous rate); the result gives a normalized rate varying between 0 and 1 (Sachs and Young 1979).

The temporal responses of the fibers were analyzed by constructing period histograms over the fundamental period of the advertisement call (10 ms), beginning after the first 10 ms of the 800 ms-long stimulus in order to reduce the influence of transients (Young and Sachs 1979). Vector strength (Goldberg and Brown 1969) was calculated from these histograms, in order to give an estimate of phase-locking to the 100 Hz fundamental. The statistical significance of phase-locking was determined using the Rayleigh test of circular data (Mardia 1972).

Synchronization of fiber firing to each individual frequency component of the complex stimulus was calculated by computing the Fourier transform of 5 copies of each period histogram (compiled using ILS signal processing software), and calculating a synchronization index based on these Fourier transforms (Johnson 1980). An example of how these calculations are performed is presented in Fig. 2. Here, the synchronization index at a particular harmonic (in this example, 100 Hz, the first harmonic) for a fiber with a CF of 152 Hz (Fig. 2A) is calculated by taking the height of the Fourier transform of the period histogram (Fig. 2B) at the 100 Hz point and dividing by the magnitude of the dc offset value (average discharge rate to the stimulus; Young and Sachs 1979). The synchronization index for this fiber at 100 Hz is then plotted along with similar data at the same harmonic for all fibers in Fig. 2C, to give a profile of population responses to one harmonic. Synchronization index varies between 0–1; it reflects the relative response at each harmonic when discharge rate is factored out (Young and Sachs 1979). The synchronization index at 100 Hz is equivalent to the vector strength of the period histogram constructed over a 10 ms period. This same analysis is then repeated for all 21 harmonics in the complex stimulus. The result (Fig. 8) is a series of plots indicating how the population of fibers phase-lock to the harmonics in the stimulus.

The representation of the entire spectrum of the complex stim-

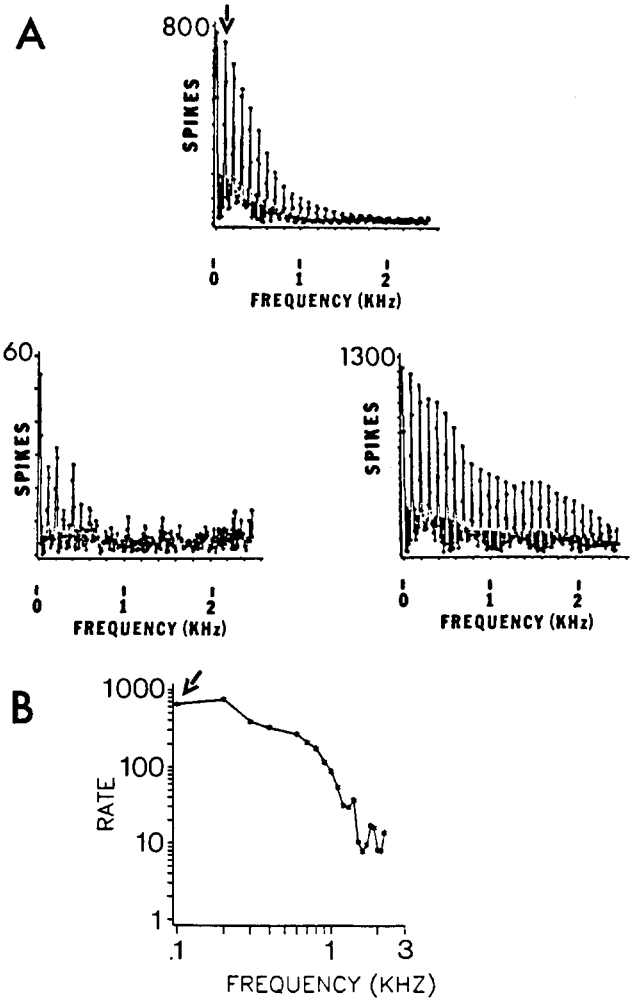

Fig. 3. Example of the steps used to calculate the average localized synchronized rate (ALSR). **A** Plots representing the Fourier transforms of the period histograms of responses of the 3 fibers with CFs falling within the critical ratio-band around 100 Hz; arrow indicates the position of the 100 Hz peak in one plot. **B** The ALSR at 100 Hz is indicated with an arrow in the bottom plot. The height of this point is the average of the 'spikes' value at 100 Hz shown in the upper 3 plots. Rate responses have been adjusted to spikes/10 s of stimulus

ulus in the overall responses of the population of fibers is illustrated in plots of 'average localized synchronized rate' (ALSR; Young and Sachs 1979). The ALSR represents the average level of synchrony to individual harmonic components of a complex sound by fibers tuned to or near to these frequency components; that is, it provides a measure of synchrony near the 'place' appropriate to a particular harmonic frequency. An example of how this measure is computed is given in Fig. 3, again for the first harmonic (100 Hz) of the stimulus. First, Fourier transforms of the period histograms for the 3 fibers whose CFs fall in a window whose width equals the approximate neural critical ratio-band around 100 Hz (Freedman et al. 1988) are computed (Fig. 3A). Then, the heights of the 100 Hz component in each of the 3 individual plots are averaged and plotted as a 'rate' measure in Fig. 3B. Responses to the 200 Hz component (second harmonic) of the stimulus are averaged over those fibers whose CFs fall in the critical ratio-band around 200 Hz, and so on. The choice of a size of an averaging window for these analyses is arbitrary; we used a window based on the size of physiological critical ratio-bands (Freedman et al. 1988) to approximate the filtering characteristics of the two auditory papillae. The shape of the ALSR profiles presented below are affected only slightly by the size of the averaging window used. Plots of ALSR contain 21 points, one point corresponding to each harmonic of the complex stimulus for 21 different groups of fibers.

Results

Data were recorded from 88 fibers of 16 bullfrogs. Fiber CFs range from 103 Hz to 2046 Hz. CF is related to threshold at CF ($r_s=0.45$, $P<0.01$); BP fibers tend to have higher thresholds than AP fibers. Thresholds to the synthetic advertisement call range from approximately 40 to 90 dB SPL and are also related to CF ($r_s=0.28$; $P<0.05$). Mean thresholds to the advertisement call are higher for BP (66 dB SPL) than for AP fibers (59 dB SPL). Call threshold and tone threshold are highly correlated ($r_s=0.74$, $P<0.01$). Spontaneous activity of fibers varies from 0–25 spikes/s. BP fibers have significantly higher mean rates of spontaneous activity than do AP fibers (5.8 as opposed to 1.2 spikes/s; normal approximation to Wilcoxon two-sample test; $z=5.3$, $P<0.001$).

Normalized average rate responses to the complex stimulus at 4 different intensities are plotted against fiber CF in Fig. 4. Since it was not possible to hold all fibers for the entire series of stimulus presentations, sample sizes differ at different stimulus intensities. At intensities of 70 and 80 dB SPL, the rate responses provide a reasonable representation of the bimodal spectral structure of the complex stimulus. There is a peak in discharge rate at low frequencies (200–300 Hz), and a dip at about 500 Hz. The high-frequency peaks occur around 700–1000 Hz, which is somewhat offset from the maximal spectral peaks at 1400–1500 Hz in the stimulus (Fig. 1). At 90 and 100 dB SPL, very little of the spectral structure of the stimulus is evident, and the response plots are relatively flat. There are no consistent differences in the rate profiles compiled separately for fibers with no and with any spontaneous activity.

Plots of period histograms from 9 representative fibers with CFs spanning the range of AP and BP tuning in response to the advertisement call presented at an intensity of 80 dB SPL are shown in Fig. 5. These histograms clearly reveal tight phase-locking to the fundamental of the complex stimulus; these histogram shapes are the most common in our data. The single-peaked shapes of the histograms do not change appreciably with stimulus intensity (Fig. 6); only the calculated vector strength varies. For those 40 fibers for which data are available at all 4 intensities, mean vector strengths are high (70 dB SPL: 0.69; 80 dB SPL: 0.79; 90 dB SPL: 0.75; 100 dB SPL: 0.66) and differ significantly ($P=0.04$; Kruskal-Wallis Test).

Over all stimulus intensities, vector strength to the 100 Hz fundamental in the complex stimulus ranges from 0.09–0.99, values which are statistically significant for all but 2 fibers. The variability in the degree of phase-locking to the fundamental of the stimulus could be ex-

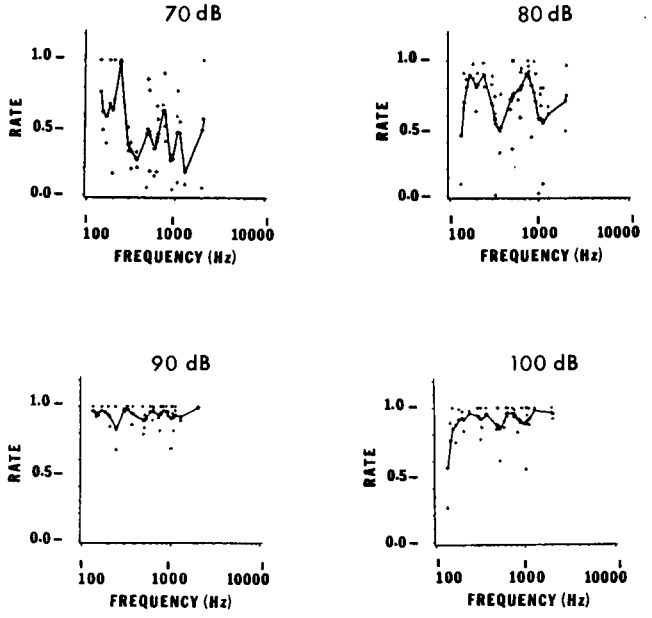

Fig. 4. Normalized average rate responses of the population of fibers to the complex stimulus presented at 4 different intensities (70, 80, 90 and 100 dB SPL), plotted against fiber CF. The line through each plot is a moving average of the points computed with a triangular weighting function with a 0.5 octave base

plained in several ways. First, BP fibers tend to show lower vector strengths than AP fibers, although this effect is statistically significant only at the highest intensity tested (100 dB SPL; $r_s=0.31$. $P<0.05$). Second, fibers with high rates of spontaneous activity tend to have lower vector strengths; this is statistically significant for vector strengths calculated at intensities of 80 ($r_s=0.31$, $P<0.05$) and 100 dB SPL ($r_s=0.42$, $P<0.01$). Third, some fibers show less synchronization at stimulus intensities close to threshold; synchronization improves at higher intensities (Fig. 7A).

Finally, the period histograms of some fibers show double peaks for at least one stimulus intensity. In some cases (Fig. 7C, D), period histograms show two peaks separated by 5 ms, an interval corresponding to the 200 Hz spectral component in the stimulus. This is the most common pattern seen in the double-peaked histograms. In other cases (Fig. 7B), the two peaks occur relatively close together. This pattern is unusual; it occurs in responses of only 7 of the total sample of fibers, and then at only one stimulus intensity. The second peak in these histograms occurs between 1.5–2.5 ms after the first peak, but these pairs of peaks are separated by about 10 ms. This pattern may represent firing to the shape of the envelope of the complex stimulus (Fig. 1B). The

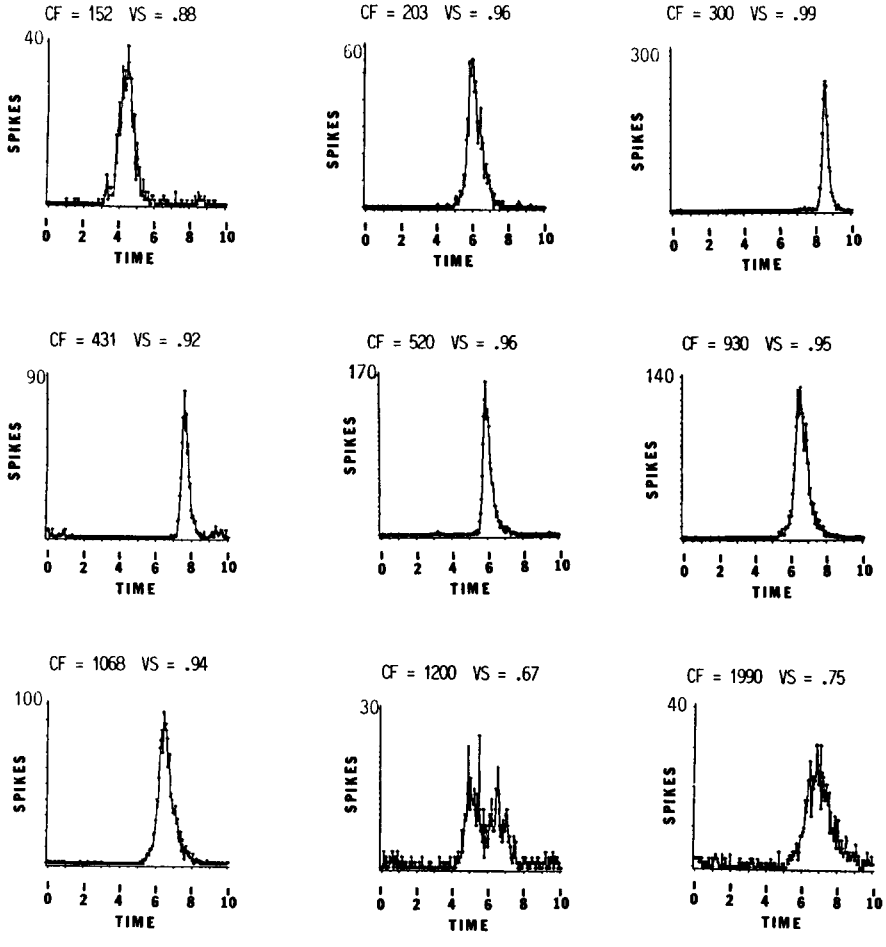

Fig. 5. Period histograms of responses of 9 fibers with different CFs to the complex stimulus presented at an intensity of 80 dB SPL. Period histograms are compiled over the 10 ms period of the fundamental. Above each plot is the fiber CF and the vector strength (VS) of the responses to the fundamental frequency

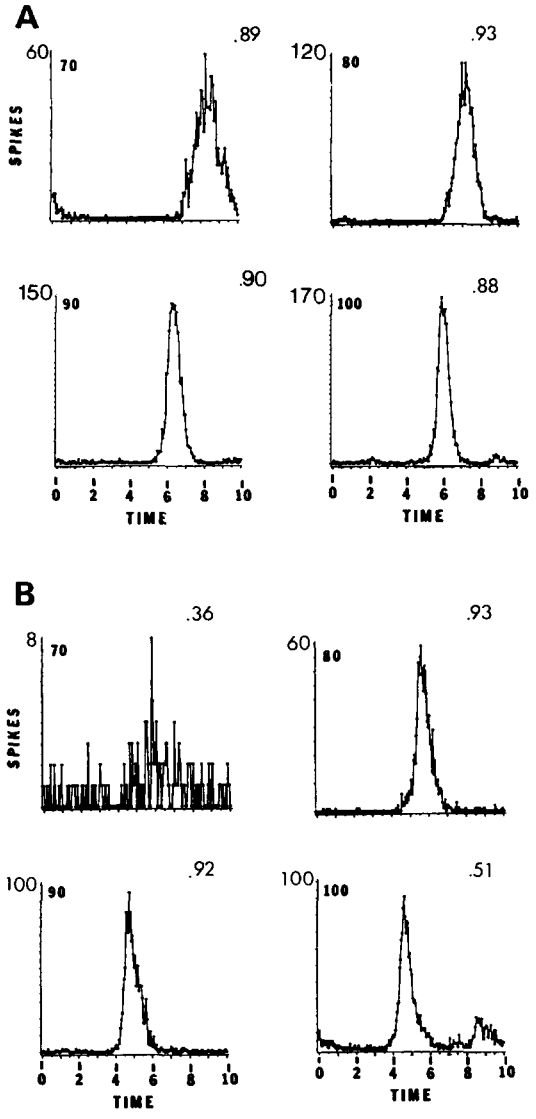

Fig. 6. Period histograms of 2 fibers in response to the synthetic advertisement call presented at 4 different intensities. **A** CF = 640 Hz. **B** CF = 1045 Hz. Number at the top left of each plot is stimulus intensity, number at the top right is the vector strength to the fundamental

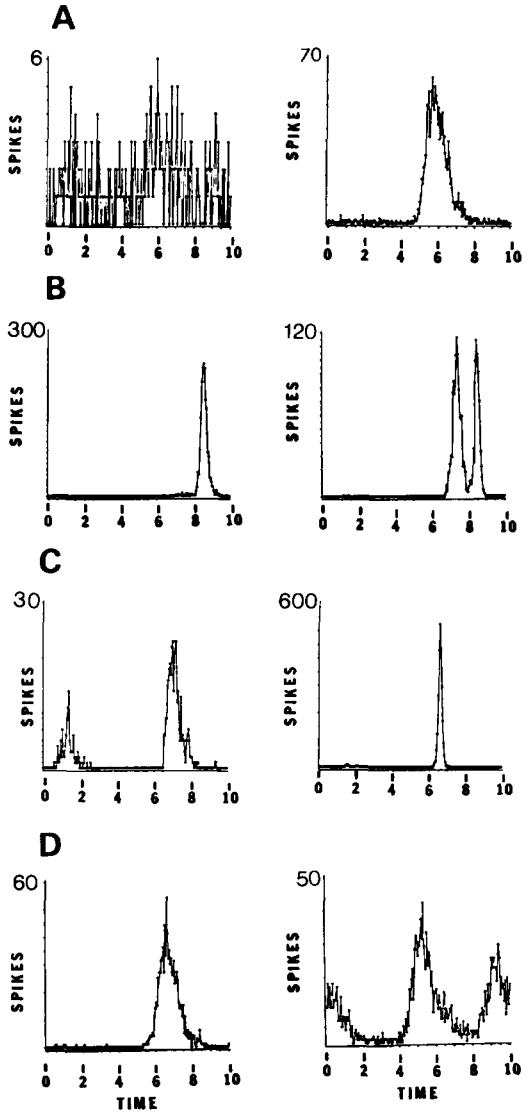

Fig. 7. Period histograms of responses to the complex stimulus for 4 fibers showing multiple peaks or a loss of good synchronization at some intensity level. **A** Fiber with CF = 1007 Hz, threshold to the complex stimulus = 80 dB SPL. Synchronization is poor at a stimulus intensity of 80 dB SPL (left) but improves at 90 dB SPL (right). **B** Fiber with CF = 300 Hz, threshold = 58 dB SPL. Period histogram shows one peak at 80 dB SPL (left) and 2 peaks at 90 dB SPL (right). **C** Fiber with CF = 320 Hz and threshold of 62 dB SPL. Period histogram shows 2 peaks separated by 5 ms intervals at 70 dB SPL (left) and 1 peak separated by 10 ms intervals at 100 dB SPL (right). **D** Fiber with CF = 1132 Hz and threshold = 60 dB SPL. Period histogram shows 1 peak at 70 dB SPL (left) and 2 peaks at 100 dB SPL (right)

appearance of double-peaked histograms is related most consistently to stimulus intensity. At low intensities (70 dB SPL), approximately 40% of the AP fibers in our sample show double-peaked histograms with peaks spaced at 5 ms intervals, which revert to the more common single-peaked shape at higher intensities (Fig. 7C; an exception is shown in Fig. 7B). At intensities of 80 dB SPL and higher, only about 20% of the sample of AP fibers have double-peaked histograms. Most (90%) BP fibers show single-peaked histograms at intensities of 70–90 dB SPL. At the highest stimulus intensity used (100 dB SPL), 60% of our sample of BP fibers develop double-peaked (Fig. 7D) period histograms, where the second peak is likely to occur at 5 ms after the first. The differences in histogram shapes of AP and BP fibers are significant at intensities of 70 ($G = 5.9$, $P < 0.05$) and 100 dB SPL ($G = 4.3$, $P < 0.05$). There are no obvious characteristics of those AP or BP fibers showing double-peaked histograms that distinguish them from those other AP or BP fibers which respond primarily to the stimulus fundamental at all intensities.

Synchronization indices calculated at the individual harmonics in the stimulus at an intensity of 80 dB SPL are plotted against fiber CF in Fig. 8. For each individual frequency component, a line representing a moving

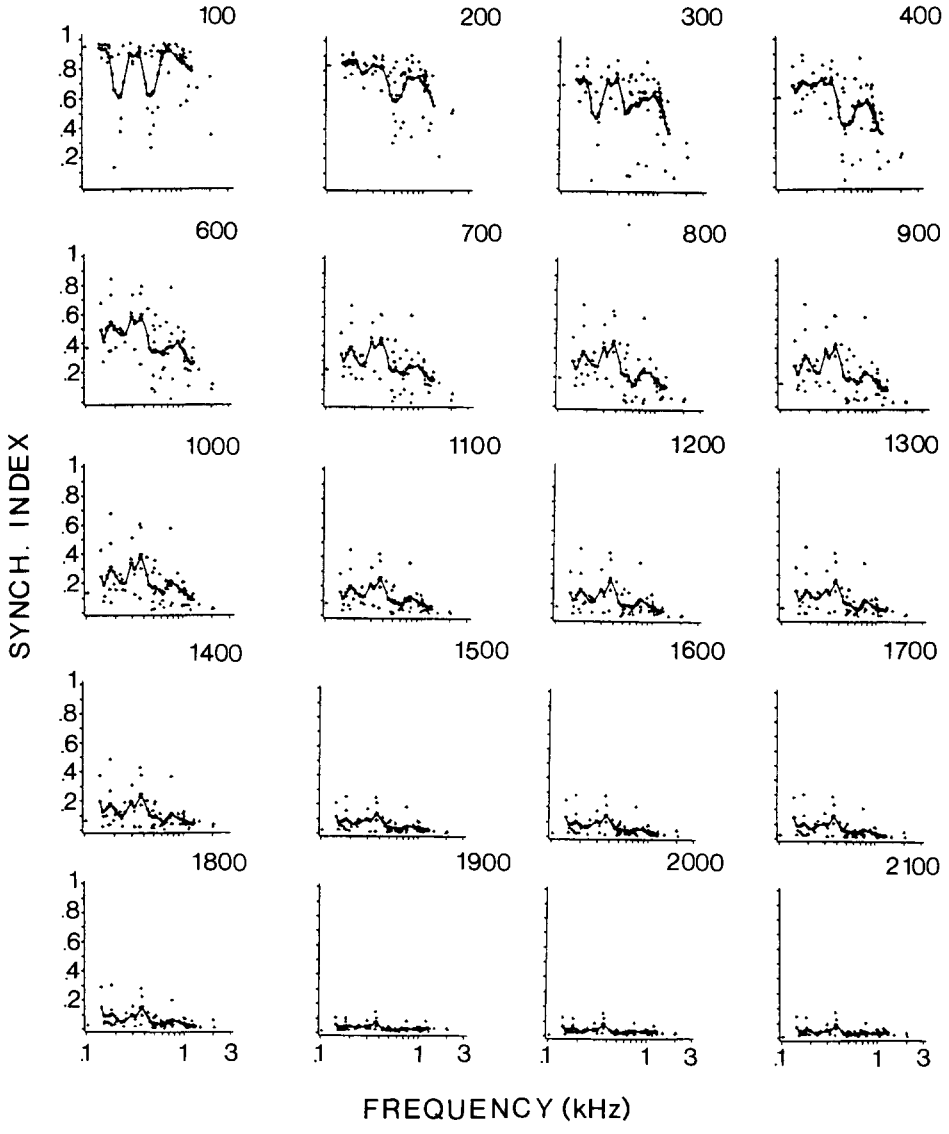

Fig. 8. Plots of synchronization index against fiber CF to 20 of the 21 components in the complex stimulus, at a stimulus intensity of 80 dB SPL. The frequency of each component is indicated above each plot. The line through each plot is a moving average of the points computed with a triangular weighting function with a 0.5 octave base

average of the individual data points using a triangular weighting function with a base of 0.5 octave is plotted. The synchronization index is higher at low frequencies than at high frequencies (the line of average indices moves closer to the abscissa with increasing frequency). This reflects a reduction in the capacity of all fibers to phase-lock to high frequencies. Even at low stimulus frequencies, BP fibers do not synchronize as well as AP fibers; these differences are significant (normal approximation to the Wilcoxon two-sample test) at frequencies of 200–2000 Hz, but not at the 100 Hz fundamental. Figure 8 shows that there is a strong synchronizing response by fibers with CFs near 100 Hz to the 100 Hz component of the stimulus. Some fibers with CFs near 200 Hz show a weaker response to 100 Hz, resulting in a dip in the average line through the data. At 200 Hz, the dominant spectral component in the stimulus, there is also a strong response by fibers tuned near 100 Hz, but now the response of all fibers with CFs near 200 Hz is particularly strong, and the dip in the average line disappears. This indicates a strong temporal response to low frequencies by fibers with CFs near those frequencies. Some fibers with CFs near 200 Hz show greater synchronization to the 200 Hz harmonic while other similarly-tuned fibers phase-lock to 100 Hz. There is also a strong response by fibers tuned near 200 Hz to 400 Hz, the fourth harmonic of the stimulus fundamental. To higher stimulus harmonics, in particular 1400 Hz, fibers with CFs near these components do not show a strong synchronizing response.

The distribution of synchronization index to the individual harmonics in the stimulus remains relatively constant with changes in stimulus intensity. This is illustrated in Fig. 9, which shows the mean synchronization index at 4 different stimulus frequencies at 4 different stimulus intensities.

The population-wide neuronal responses at the 4 different stimulus intensities are illustrated in plots of ALSR (Fig. 10). These plots reveal the reduction in synchronization with increasing harmonic frequency. That is, they reflect the low-pass characteristics of the temporal response of anuran eighth nerve fibers. The ALSR

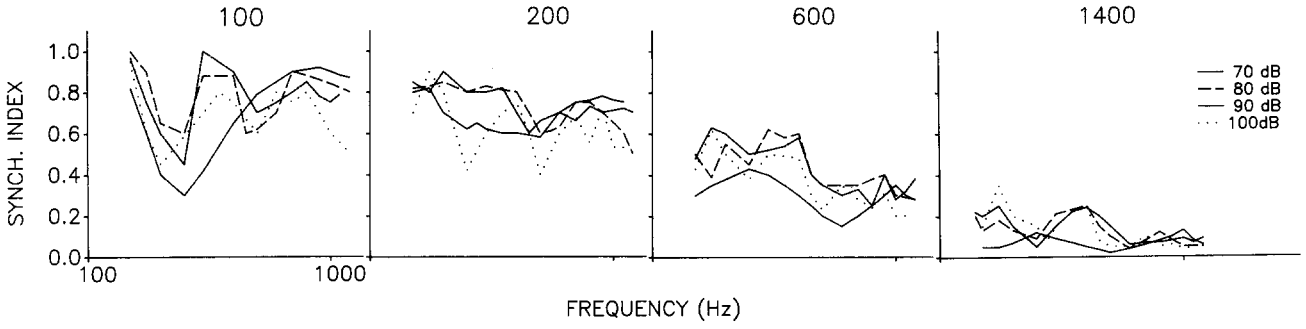

Fig. 9. Plots of mean synchronization index, using a moving weighted average of the data points, at 100, 200, 600, and 1400 Hz at 4 different stimulus intensities

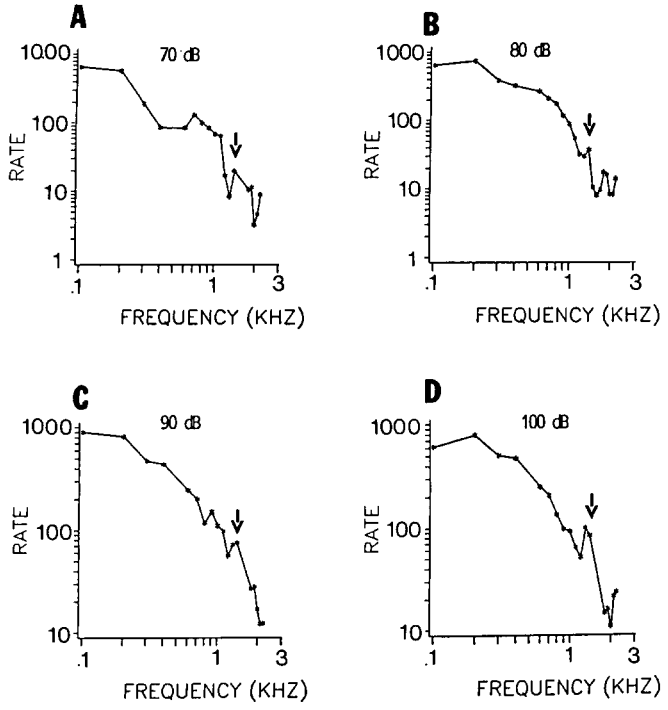

Fig. 10. A–D Plots of average localized synchronized rate to the complex stimulus at intensities of 70, 80, 90 and 100 dB SPL. Arrow indicates the values at 1400 Hz. Rate responses have been adjusted to spikes/10 s of stimulus

plots also reveal some of the spectral complexity in the bullfrog advertisement call. Note the high rates at both 100 and 200 Hz, corresponding to the frequency of the fundamental and the 200 Hz peak in the call. Note also the small secondary peak at 1400 Hz which is the location of the upper spectral peak in the stimulus. However, except for the 70 dB plot, there is no evident dip in the mid-frequency region (500 Hz) as appears in the stimulus. The shapes of the ALSR plots are fairly similar for the 4 stimulus intensities, and the effects of rate saturation are not as obvious as in plots of average discharge rate (Fig. 5).

Discussion

Most bullfrog eighth nerve fibers phase-lock strongly to the species-specific advertisement call at a periodicity equal to that of the temporal envelope of the call. These fibers synchronize exclusively to the fundamental frequency of the complex stimulus at all stimulus intensities. What varies is the magnitude of the synchronization (vector strength). The underlying spectral complexity of the stimulus is not accurately reflected in the timing of fiber firing. Synchronization to the other harmonics in the stimulus is not evident in the period histograms of fiber responses. A small number of fibers show synchronization to the low-frequency spectral energy in the stimulus, and, for most of these fibers, these effects depend on stimulus intensity. There is little evidence of synchronization at periods corresponding to the high-frequency spectral energy in the stimulus.

The generally poor synchronizing response to high frequencies seen here is consistent with data from the few other studies which have examined phase-locking in the anuran auditory periphery. In contrast with mammalian auditory nerve fibers, which can show significant phase-locking to frequencies up to 5000 Hz (Rose et al. 1967), anuran fibers do not phase-lock to CF tones above 700–1000 Hz (Freedman et al. 1988; Hillery and Narins 1987; Narins and Wagner 1989; Narins and Hillery 1983). Phase-locking at CF is more characteristic of AP than of BP fibers. BP fibers show significant phase-locking to low frequency tone-bursts within their tuning curves (Narins 1987; Narins and Wagner 1989). It is unlikely that the strong synchronization to the fundamental of the complex stimulus by BP fibers shown here is simply the result of these fibers phase-locking to frequencies of 100 Hz in their tuning curves. Even at the highest intensity presented (100 dB SPL), most BP fibers do not respond to single tone-bursts of 100 Hz. Rather, we suggest that BP fibers are, in effect, responding to the 'missing fundamental' derived from those high-frequencies in the complex stimulus which are within the range of BP tuning. Coupled with the broad tuning of BP fibers, these effects suggest that the BP acts like a temporal filter for detection of periodicity or 'pitch'. The sensitivity of the BP to waveform periodicity was also seen in previous work (Frishkopf and Goldstein 1963; Rose and Capranica 1985). Rose and Capranica (1985) reported that BP fibers show more

robust phase-locking to the envelope of amplitude-modulated noise than do AP fibers. Although we have confirmed the sensitivity of the BP to stimulus periodicity, in our study, BP fibers tend to show somewhat less synchronization to the harmonics of the complex stimulus than do AP fibers (Fig. 8), but there are no significant differences in synchronization to the fundamental frequency except at the highest stimulus intensity tested.

Strong phase-locking of responses to the fundamental frequency of the complex stimulus is relatively immune to changes in stimulus intensity. At stimulus intensities producing rate saturation, significant phase-locking to the fundamental frequency still occurs; only the calculated vector strength varies. Temporal coding of simple stimuli is also relatively more immune to the effects of stimulus intensity and background noise than is rate coding (Freedman et al. 1988; Narins and Wagner 1989). Therefore, the dynamic range problem (Evans 1981) may not be a particularly serious one for accurate encoding of the periodicity present in natural calls. This is important because the different functional categories of vocalizations used by many species of anurans often differ in pulse repetition rate. These different call types may also differ in the intensity levels over which they are most often used. For example, in some neotropical treefrogs, aggressive calls are usually employed in close-range encounters while advertisement calls predominate between more widely-spaced individuals (Schwartz and Wells 1984). The pulse repetition rate (periodicity) of aggressive calls in these species is higher than those of advertisement calls. Psychophysical studies (Simmons 1988) also suggest that anurans are quite sensitive to periodicity cues in complex sounds, and may use waveform periodicity as a means of improving the signal-to-noise ratio for detection.

The stereotyped nature of the responses of the population of fibers to the fundamental frequency of the complex stimulus is a striking finding of our study. This effect is independent of CF, and implies similarity of processing between the two peripheral auditory organs. This finding differs from results reported in studies of coding of speech sounds in the mammalian auditory nerve. Period histograms of responses of mammalian eighth nerve fibers to synthetic speech sounds usually show multiple peaks. These peaks can correspond to the fundamental frequency, the CF of the fiber, or harmonics of the fundamental frequency close to one of the formants (predominant spectral peaks) in the stimulus (Delgutte and Kiang 1984a; Miller and Sachs 1984; Sinex and Geisler 1983; Young and Sachs 1979). Rate suppression and nonlinear effects also contribute to these responses in the mammalian auditory nerve (Sachs and Young 1980).

It is unclear how nonlinearities affect the synchronized responses of anuran eighth nerve fibers. AP, but not BP, fibers respond to quadratic difference tones (f2-f1; f2>f1); and only low-frequency-sensitive AP fibers are sensitive to two-tone suppression (Capranica and Moffat 1980). In spite of these differences between the two papillae in their sensitivity to these kinds of nonlinearities, fibers from these two organs respond similarly to the complex stimulus; therefore, it is unlikely that these nonlinearities contribute significantly to the pattern of results seen. We modelled the relative contribution of quadratic distortion products in our data by first calculating the location of each difference tone for the complex stimulus, using the empirical results of Capranica and Moffat (1980) to estimate the effect of both intensity differences and frequency separation of the primary tones in our stimulus on relative firing rate. The results of this simple model show a maximum effect at 100 Hz and a sharp dropoff at higher frequencies. Therefore, at 100 Hz the contribution of intermodulation distortion may simply supplement the strong response to the fundamental frequency of the advertisement call. At other frequencies, it is likely this nonlinearity is so much weaker than the effect of the primary harmonic components that its impact on firing rate is insignificant.

One focus of this experiment was to examine the relative precision of coding of the complex spectral structure of the synthetic advertisement call by a rate and by a temporal code. At intensities of 70–80 dB SPL, rate responses provide a fairly good representation of the stimulus, particularly in the low- and mid-frequency range (Fig. 4). At high frequencies, however, the peak in the rate plots is somewhat lower than that in the stimulus, and the position of the high frequency peaks varies somewhat at these two intensities. Some of this variability may be related to the relatively small number (17) of BP fibers in our sample. At higher intensities, the normalized rate response saturates. In our study, most (72%) fibers reach rate saturation at advertisement call intensities of 90 dB SPL. Therefore, even though we recorded from fibers with a range of thresholds, the population still shows evidence of rate saturation at high intensities. The rate profiles of mammalian auditory nerve fibers likewise show a good representation of the spectral structure of synthetic vowel sounds only at low and moderate intensities (Sachs and Young 1979). Spontaneous rate is an important factor influencing responses of mammalian fibers to complex sounds (Carney and Geisler 1986; Geisler and Gamble 1989; Sachs and Young 1979; Sachs et al. 1983). Low spontaneous rate mammalian fibers can retain formant peaks in rate profiles at higher intensities than high spontaneous rate fibers (Sachs and Young 1980). Dividing our data by spontaneous rate and calculating rate profiles separately on the basis of this variable do not provide more accurate representation of the structure of the stimulus at any intensity level. This is probably because of the small number of fibers in these two subsets, and because anuran eighth nerve fibers show much less spontaneous activity than do mammalian fibers.

Plots of synchronization index over CF (Figs. 8, 9) show how well fibers synchronize to any particular frequency (harmonic) component in the stimulus. They essentially show that the synchronization index is higher at low than at high harmonics, and that BP fibers do not synchronize as well as AP fibers. At stimulus frequencies above about 1400 Hz, there is very little pattern

in these plots. At lower harmonics, peaks corresponding to the fundamental frequency, the low-frequency spectral peak, and the high-frequency spectral peak in the stimulus are present. These calculations of synchronization index are based on Fourier transforms of the period histograms (Fig. 2). The frequency composition of the spectrum reflects the shape of the histogram peak; however, the sharpness of this peak is not necessarily an index of the high-frequency limits of synchronization in the bullfrog (Freedman et al. 1988). Period histograms are rectified waveforms, so Fourier transforms of them can show energy at harmonics of the fundamental when none actually exists in the stimulus. The interpretation of the spectrum must therefore be done with caution, because frequencies may be present in the spectrum due to the shape of the peak without their being present in the period of neural discharges (Sachs and Young 1980). For these kinds of data, the question then arises as to which components in the Fourier transform are the results of rectifier distortion and which are instead responses to stimulus frequencies (which also occur at harmonics of the fundamental), or both. The Fourier transforms of the period histograms compiled here generally show significant energy at integer multiples of the fundamental frequency, even though the histograms themselves show only one peak, corresponding to the fundamental frequency. Because there is a spectral notch in the stimulus at frequencies of 500 Hz (Fig. 1), it is clear that apparent peaks in the Fourier transform at this frequency and its harmonics are the results of rectification. Rectifier distortion products should follow the distribution of the primary responses from which they are generated (Sachs and Young 1980). In Fig. 8, responses to frequencies of 200–1400 Hz generally follow the pattern shown to the 100 Hz component; simply the absolute value of the synchronization index at these frequencies varies. It is likely that many responses to frequencies above 100 Hz are really distortion products of the 100 Hz response; however, because some fibers synchronize to the 200 Hz harmonic in the stimulus, responses at this frequency might reflect both rectification distortion and 'true' neuronal firing patterns.

The ALSR incorporates rate, place, and timing information. Plots of this measure of population-wide response (Fig. 10) have a similar low-pass shape, and might reveal some of the underlying spectral complexity present in the bullfrog advertisement call. In particular, the 100 Hz, 200 Hz, and 1400 Hz components are evident as a response peak at all four stimulus intensities. Since bullfrog eighth nerve fibers fail to show significant phase-locking to tone bursts at 1400 Hz (Freedman et al. 1988), this peak is certainly a result of the high rate response of fibers with CFs near 1400 Hz. The nearly identical appearance of the response plots for 70, 80, 90, and 100 dB SPL stimuli suggests that the ALSR could provide important information on spectral structure at stimulus intensities where rate information alone is inadequate. On the other hand, ALSR plots show high values in the mid-frequency range where there is no spectral energy in the stimulus (Fig. 1), and also at other frequencies, which, though present in the stimulus, are not reflected in the period histograms. The low-pass shapes of these ALSR plots are affected by rectifier distortion arising from Fourier transforms of single-peaked period histograms (Young and Sachs 1980). This is particularly obvious in the mid-frequency range, where there is little spectral energy in the stimulus, but also contributes to the pattern of results at other frequencies as well.

Whether the central nervous system is capable of performing a calculation analogous to that used to compute the ALSR is not known. There are two fundamental steps in this calculation: (1) central auditory neurons must isolate from groups of fibers with similar CFs the component at or close to CF, and (2) a phase reference for the stimulus is necessary to compute period histograms (Young and Sachs 1979). In their discussion of this issue, Young and Sachs point out that (1) is theoretically possible given the short interaural time delays which central neurons can detect. While (2) is unlikely, a cross-correlation mechanism (e.g. Licklider 1951) operating on eighth nerve fiber spike trains could provide the same information as the ALSR since the Fourier transform of the interval histogram of fiber discharges is close to the power spectrum of their period histogram (Young and Sachs 1979). Other processes, such as the dominant component scheme discussed by Delgutte (1984), may also be relevant to understanding complex sound processing in the anuran's peripheral auditory system. This scheme relies upon a central Fourier analysis to detect dominant periodicities in the response patterns of eighth nerve fibers. Because it, as well as the ALSR, relies on a peripheral place coding mechanism, this scheme might not adequately account for processing in an auditory organ not organized tonotopically, such as the BP. In any event, more data on complex sound processing in the anuran periphery need to be collected before models of such processing can be devised.

From these data, we suggest that neither rate profiles nor the ALSR alone provide an accurate representation of spectral and temporal structure of the complex advertisement call. ALSR plots might be somewhat more useful because they are relatively invariant to stimulus intensity. It is interesting to note, however, that bullfrogs tested in an evoked calling paradigm respond most consistently to synthetic advertisement calls presented at intensities of 80 dB SPL than to more or less intense stimuli (Megela-Simmons 1984). This is an intensity level at which rate profiles provide a rather good representation of the advertisement call. The results of this experiment also suggest that the periphery is transmitting complex spectral information through arrays of phase-locked activity. This tight encoding of activity is necessary for analysis of periodicity cues by temporally-tuned neurons in the auditory midbrain (Rose and Capranica 1985).

Acknowledgments. This research was supported by NIH grants NS08285 to JJS and NS21911 to AMS.

References

Capranica RR (1965) The evoked vocal response of the bullfrog: a study of communication by sound. Res Monogr 33. M.I.T. Press, Cambridge, Massachusetts

Capranica RR (1968) The vocal repertoire of the bullfrog (*Rana catesbeiana*). Behaviour 31:302–325

Capranica RR, Moffat AJM (1980) Nonlinear properties of the peripheral auditory system of anurans. In: Popper AN, Fay RR (eds) Comparative studies of hearing in vertebrates. Springer, Berlin Heidelberg New York, pp 139–165

Capranica RR, Moffat AJM (1983) Neurobehavioral correlates of sound communication in anurans. In: Ewert J-P, Capranica RR, Ingle DJ (eds) Advances in vertebrate neuroethology. Plenum, New York, pp 701–730

Carney LH, Geisler CD (1986) A temporal analysis of auditory-nerve fiber responses to spoken stop consonant-vowel syllables. J Acoust Soc Am 79:1896–1914

Davis MS (1987) Acoustically mediated neighbor recognition in the North American bullfrog, *Rana catesbeiana*. Behav Ecol Sociobiol 21:185–190

Delgutte B (1984) Speech coding in the auditory nerve: II. Processing schemes for vowel-like sounds. J Acoust Soc Am 75:879–886

Delgutte B, Kiang NYS (1984a) Speech coding in the auditory nerve. I. Vowel-like sounds. J Acoust Soc Am 75:866–878

Delgutte B, Kiang NYS (1984b) Speech coding in the auditory nerve: III. Voiceless fricative consonants. J Acoust Soc Am 75:887–896

Evans EF (1981) The dynamic range problem: place and time coding at the level of the cochlear nerve and nucleus. In: Syka J, Aitken L (eds) Neuronal mechanisms of hearing. Plenum Press, New York, pp 69–85

Feng AS (1982) Quantitative analysis of intensity-rate and intensity-latency functions in peripheral auditory nerve fibers of northern leopard frogs (*Rana p. pipiens*). Hear Res 6:241–246

Feng AS, Narins PM, Capranica RR (1975) Three populations of primary auditory fibers in the bullfrog (*Rana catesbeiana*): their peripheral origins and frequency sensitivities. J Comp Physiol 100:221–229

Freedman EG, Ferragamo M, Simmons AM (1988) Masking patterns in the bullfrog (*Rana catesbeiana*). II. Physiological effects. J Acoust Soc Am 84:2081–2091

Frishkopf LS, Goldstein MH (1963) Responses to acoustic stimuli from single units in the eighth nerve of the bullfrog. J Acoust Soc Am 35:1219–1228

Geisler CD, Gamble T (1989) Responses of 'high-spontaneous' auditory-nerve fibers to consonant-vowel syllables in noise. J Acoust Soc Am 85:1639–1652

Goldberg JM, Brown PB (1969) Response of binaural neurons of dog superior olivary complex to dichotic tonal stimuli: Some physiological mechanisms of sound localization. J Neurophysiol 32:613–636

Hillery CM, Narins PM (1987) Frequency and time domain comparison of low-frequency auditory fiber responses in two anuran amphibians. Hear Res 25:233–248

Johnson DH (1980) The relationship between spike rate and synchrony in responses of auditory-nerve fibers to single tones. J Acoust Soc Am 68:1115–1122

Lewis ER, Leverenz EL, Koyama H (1982) The tonotopic organization of the bullfrog amphibian papilla, an auditory organ lacking a basilar membrane. J Comp Physiol 145:437–445

Licklider JCR (1951) A duplex theory of pitch perception. Experientia 7:128–134

Mardia KV (1972) Statistics of directional data. Academic, London

Megela Simmons A (1984) Behavioral vocal response thresholds to mating calls in the bullfrog, *Rana catesbeiana*. J Acoust Soc Am 76:676–681

Megela AL, Capranica RR (1981) Response patterns to tone bursts in peripheral auditory system of anurans. J Neurophysiol 46:465–478

Miller MI, Sachs MB (1983) Representation of stop consonants in the discharge patterns of auditory-nerve fibers. J Acoust Soc Am 74:502–517

Miller MI, Sachs MB (1984) Representation of voice pitch in discharge patterns of auditory-nerve fibers. Hear Res 14:257–279

Narins PM (1987) Coding of signals in noise by amphibian auditory nerve fibers. Hear Res 26:145–154

Narins PM, Hillery CM (1983) Frequency coding in the inner ear of anuran amphibians. In: Klinke R, Hartmann R (eds) Hearing – Physiological bases and psychophysics. Springer, Berlin Heidelberg New York, pp 70–76

Narins PM, Wagner I (1989) Noise susceptibility and immunity of phase locking in amphibian auditory-nerve fibers. J Acoust Soc Am 85:1255–1265

Rose GJ, Capranica RR (1985) Sensitivity to amplitude modulated sounds in the anuran auditory nervous system. J Neurophysiol 53:446–465

Rose JE, Brugge JF, Anderson DJ, Hind JE (1967) Phase-locked response to low-frequency tones in single auditory nerve fibers of the squirrel monkey. J Neurophysiol 30:769–793

Sachs MB, Young ED (1979) Encoding of steady-state vowels in the auditory nerve: Representation in terms of discharge rate. J Acoust Soc Am 66:470–479

Sachs MB, Young ED (1980) Effects of nonlinearities on speech encoding in the auditory nerve. J Acoust Soc Am 68:858–875

Sachs MB, Voigt HF, Young ED (1983) Auditory nerve representation of vowels in background noise. J Neurophysiol 50:27–45

Schwartz JJ, Wells KD (1984) Interspecific acoustic interactions of the neotropical treefrog *Hyla ebraccata*. Behav Ecol Sociobiol 14:211–224

Simmons AM (1988) Selectivity for harmonic structure in complex sounds by the green treefrog (*Hyla cinerea*). J Comp Physiol A 162:397–403

Sinex D, Geisler CD (1983) Responses of auditory-nerve fibers to consonant-vowel syllables. J Acoust Soc Am 73:602–615

Wiewandt TA (1969) Vocalization, aggressive behavior, and territoriality in the bullfrog, *Rana catesbeiana*. Copeia 1969:276–285

Young ED, Sachs MB (1979) Representation of steady-state vowels in the temporal aspects of the discharge patterns of populations of auditory-nerve fibers. J Acoust Soc Am 66:1381–1403

Zakon HH, Wilczynski W (1988) The physiology of the anuran eighth nerve. In: Fritzsch B, Ryan MJ, Wilczynski W, Hetherington TE, Walkowiak W (eds) The evolution of the amphibian auditory system. Wiley Interscience, New York, pp 125–155

Zelick R, Narins PM (1985) Temporary threshold shift, adaptation, and recovery characteristics of frog auditory nerve fibers. Hear Res 17:161–176